Heliyon 10 (2024) e34877

Contents lists available at ScienceDirect

Heliyon

journal homepage: www.cell.com/heliyon

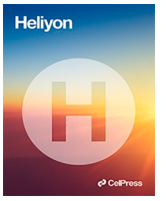

Research article

Predicting CTLA4 expression and prognosis in clear cell renal cell carcinoma using a pathomics signature of histopathological images and machine learning

Xiaoqun Yang [a,1], Xiangyun Li [a,1], Haimin Xu [a,1], Silin Du [b], Chaofu Wang [a], Hongchao He [c,d,*]

[a] Department of Pathology, Shanghai Ruijin Hospital, Shanghai Jiaotong University School of Medicine, Shanghai, China
[b] University Hospital, Shanghai Jiaotong University, Shanghai, China
[c] Department of Urology, Shanghai Ruijin Hospital, Shanghai Jiaotong University School of Medicine, Shanghai, China
[d] Department of Genitourinary Medical Oncology, The University of Texas MD Anderson Cancer Center, Houston, TX, 77030, USA

ARTICLE INFO

Keywords:
Pathomics signature
CTLA4
Machine learning
Clear cell renal cell carcinoma

ABSTRACT

Background: CTLA4, an immune checkpoint, plays an important role in tumor immunotherapy. The purpose of this study was to develop a pathomics signature to evaluate CTLA4 expression and predict clinical outcomes in clear cell renal cell carcinoma (ccRCC) patients.

Methods: A total of 354 patients from the TCGA-KIRC dataset were enrolled in this study. The patients were stratified into two groups based on the level of CTLA4 expression, and overall survival rates were analyzed between groups. Pathological features were identified using machine learning algorithms, and a gradient boosting machine (GBM) was employed to construct the pathomics signatures for predicting prognosis and CTLA4 expression. The predictive performance of the model was subsequently assessed. Enrichment analysis was performed on diferentially expressed genes related to the pathomics score (PS). Additionally, correlations between PS and TMB, as well as immune infiltration profiles associated with different PS values, were explored. *In vitro* experiments, CTLA4 knockdown was performed to investigate its impact on cell proliferation, migration, invasion, TGF-β signaling pathway, and macrophage polarization.

Results: High expression of CTLA4 was associated with an unfavorable prognosis in ccRCC patients. The pathomics signature displayed good performance in the validation set (AUC = 0.737; $P < 0.001$ in the log-rank test). The PS was positively correlated with CTLA4 expression. We next explored the underlying mechanism and found the associations between the pathomics signature and TGF-β signaling pathways, TMB, and Tregs. Further *in vitro* experiments demonstrated that CTLA4 knockdown inhibited cell proliferation, migration, invasion, TGF-β expression, and macrophage M2 polarization.

Conclusion: High expression of CTLA4 was found to correlate with poor prognosis in ccRCC patients. The pathomics signature established by our group using machine learning effectively predicted both patient prognosis and CTLA4 expression levels in ccRCC cases.

* Corresponding author. Department of Urology, Shanghai Ruijin Hospital, Shanghai Jiaotong University School of Medicine, Shanghai, China.
E-mail address: hhc11775@rjh.com.cn (H. He).
[1] Contribute equally.

https://doi.org/10.1016/j.heliyon.2024.e34877
Received 8 August 2023; Received in revised form 15 July 2024; Accepted 17 July 2024
Available online 18 July 2024

1. Introduction

Clear cell renal cell carcinoma (ccRCC) is a malignant tumor originated from the proximal tubular epithelial cells and represents the predominant histological type of renal cell carcinoma, accounting for more than 75 % of cases [1]. Despite treatment advances, the prognosis remains poor, especially in patients with advanced ccRCC [2]. Several potential prognostic markers have been identified, including VHL [3,4], PBRM1 [5], and transcriptomic signatures [6,7]. However, they have yet to be integrated into routine clinical practice as definitive indicators. As a result, the prognosis of ccRCC currently relies mainly on imaging and tumor-node-metastasis (TNM) staging, lacking reliable prognostic tools for clinical application [8]. Therefore, there is an urgent need to investigate new prognostic markers to stratify patient prognosis and provide precise and personalized treatment regimens in the near future.

It has been demonstrated that ccRCCs exhibit a high degree of immune infiltration. Immune checkpoint blockade (ICB) therapy and combination regimens have shown significant improvement in the survival rates of ccRCC patients [9,10]. Cytotoxic T Lymphocyte-associated Antigen-4 (CTLA4), also known as differentiation cluster 152 (CD152), is an immune checkpoint protein receptor involved in immune response regulation. It is increasingly utilized in immune modulation strategies for cancer treatment [11]. Multiple studies have suggested that CTLA4 may serve as a potential prognostic or predictive biomarker for ccRCC [12], showing promising application prospects in tumor therapy [13,14]. However, current methods for detecting CTLA4 expression levels still have limitations [15].

Pathomics refers to the transformation of pathological images into high-fidelity and high-throughput data that can be mined based

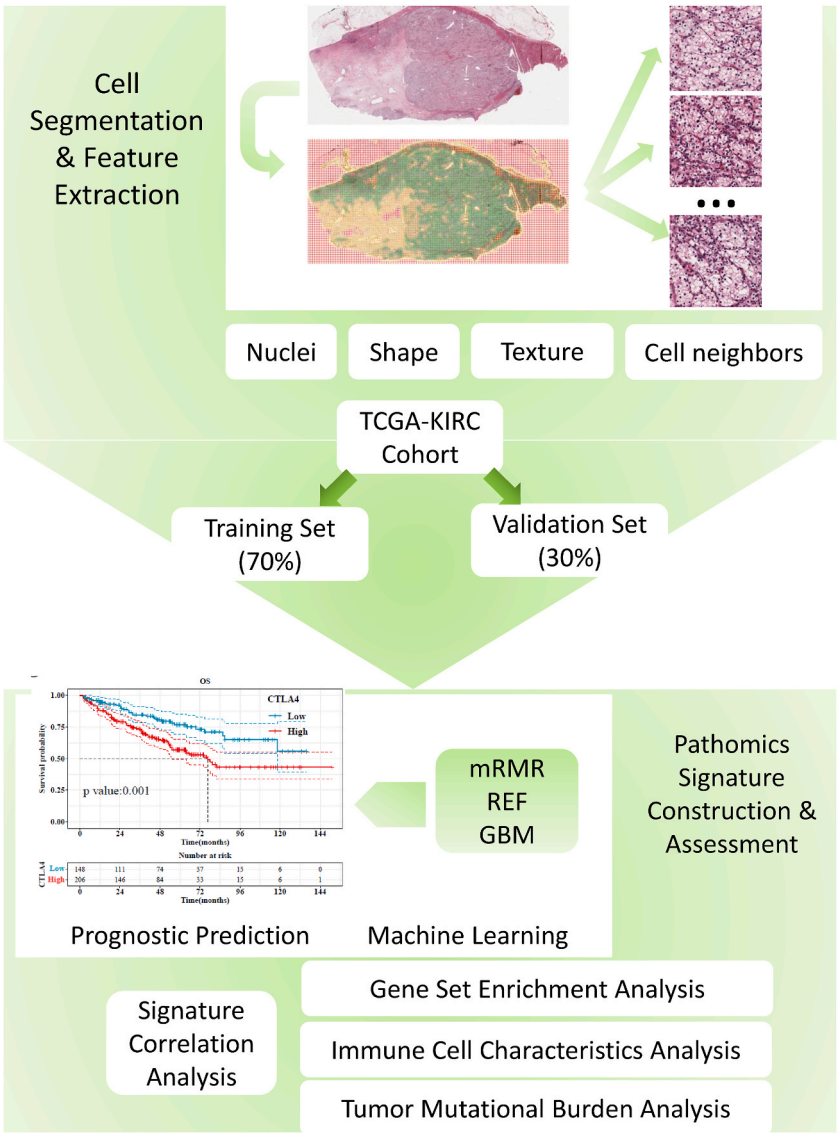

Fig. 1. Flow chart of the whole work.

on artificial intelligence, covering quantitative features such as texture features, morphological features, edge gradient features, and biological characteristics. This approach enables the quantification of pathological diagnosis, molecular expression, and disease prognosis [16–18]. In this study, the histopathological images of ccRCC patients were collected, and a survival-related pathological feature was constructed by using machine learning to predict the expression and prognosis of CTLA4 in ccRCC patients.

2. Methods and materials

2.1. Patient cohorts

The study enrolled 354 samples of ccRCC patients from TCGA-KIRC dataset. The criteria for selecting these samples were as follows: (a) screening samples with preliminary diagnosis and treatment; (b) the survival time of the patient is greater than 1 month; (c) Samples with simultaneous clinical data, primary solid tumors, and RNA sequences; (d) images of acceptable quality.

2.2. Image acquisition and segmentation

Histopathological images (20 × or 40 × magnification) stained with hematoxylin and eosin (H&E) were downloaded from the TCGA database (https://tcga-data.nci.nih.gov/tcga/) [19,20]. The OTSU algorithm (https://opencv.org/) was employed to segment the tissue area by applying a threshold value to separate the unnecessary background from the relevant organizational area for research [21]. The 40 × images were divided into multiple sub-images of size 1024 × 1024 pixels, while the 20 × images were divided into multiple sub-images of size 512 × 512 pixels. Pathologists reviewed all sub-images to remove poor-quality images, including those with contamination, blurriness, or more than 50 % blank space. From each pathological image, 10 sub-images were randomly selected for subsequent analysis [19,20].

2.3. Feature extraction

PyRadiomics open-source packages (https://pyradiomics.readthedocs.io/en/latest/) was used for the standardization of each sub-image. PyRadiomics open-source packages extracted a total of 1488 features, including 93 original features (first-order and second-order features), higher-order features (Wavelet LL, Wavelet LH, Wavelet Hl and Wavelet HH) and LoG ((kernel size: 1, 2, 3, 4, 5), Square, SquareRoot, Logarithm, Exponential, Gradient and LBP2D).

After extracting features from the 10 sub-images of each pathological image, the corresponding average value was calculated to obtain the pathomic features for each sample, which were used for subsequent data analysis [17,22,23].

2.4. Prediction models of CTLA4 expression and assessment

The samples were randomly divided into the training set and the verification set according to the ratio of 7:3, and the process is shown in Fig. 1. The training set was used to construct pathological features, while the validation set was used to evaluate the model. Features were filtered by using the maximum correlation, Minimum redundancy (mRMR) algorithm, which considers not only the correlation between the features and the variables to be predicted, but also the correlation between the features. Before modeling, in order to find a subset of predictors that can be used to generate an accurate model, the predictors were ranked using Recursive Feature Elimination (RFE) feature filtering and less important predictors were removed in order. The Gradient Boosting Machine (GBM) was used to model selected pathological features to predict ccRCC patient survival.

The evaluation of the prediction models was based on several performance measures, including accuracy, specificity, sensitivity, positive predictive value (PPV), and negative predictive value (NPV). The predictive performance of the models was assessed using Receiver Operating Characteristic Curve (ROC) analysis. The calibration of the pathomics prediction model was evaluated by generating a calibration curve. Additionally, Decision Curve Analysis (DCA) was conducted to illustrate the clinical benefits of the pathomics prediction model. The main packages employed in the analysis were "pROC", "measures", "ResourceSelection", "rms", and "rmda" in R software.

2.5. Differentially expressed genes enrichment analysis

To investigate the underlying molecular mechanism behind the differential expression observed between high and low expression groups in the pathomics score (PS), we performed Gene Set Enrichment Analysis (GSEA). Differentially expressed genes (DEGs) between the high and low PS groups were analyzed using the "clusterProfiler" package in R software. We focused on the top 30 channels in both the KEGG database and HALLMARK database. A statistical significance threshold of $P < 0.05$ was applied to determine significant enrichment.

2.6. Correlation analysis of tumor mutation burden (TMB)

Maf format mutation data was downloaded from TCGA database (https://portal.gdc.cancer.gov/). Correlation analysis was performed using the 'corrplot' package in R software.

2.7. Immunocytes infiltration analysis

The gene expression matrix of ccRCC samples were uploaded to the CIBERSORTx database (https://cibersortx.stanford.edu/). The infiltration of immune cells was calculated in each sample. The difference between high PS expression group and low PS expression group and the degree of immune cell infiltration were analyzed.

2.8. Cell culture and transfection

The human renal clear cell carcinoma cell line Caki1 was procured from the cell bank of the Chinese Academy of Sciences (Shanghai, China). Cells were cultured in McCoy's 5A medium (Gibco) supplemented with 10 % FBS (Gibco) and 1 % P/S (Gibco) at 37 °C in a 5 % CO_2 incubator. Subconfluent cells were selected for subsequent functional studies. THP-1 monocytes were cultured in RPMI medium supplemented with 10 % FBS. To induce differentiation into macrophages, 12-*O*-tetradecanoylphorbol-13-acetate (PMA, 100 ng/ml, Solarbio, China) was added to THP-1 monocytes. Small interfering RNAs (siCTLA4) for CTLA4 knockdown and control (NC) siRNA were provided by Genomeditech (Shanghai, China) and transfected into cells using Lipofectamine 3000 (Invitrogen), following the manufacturer's instructions.

2.9. Cell Counting Kit-8 (CCK-8) and transwell assay

For the CCK-8 assay, cells were seeded in triplicate into 96-well plates. CCK-8 solution (10 μL) was added to each well, and the cells were incubated in the dark at 37 °C. Optical density (OD) values at 450 nm were measured at 0, 24, 48, and 72 h using a

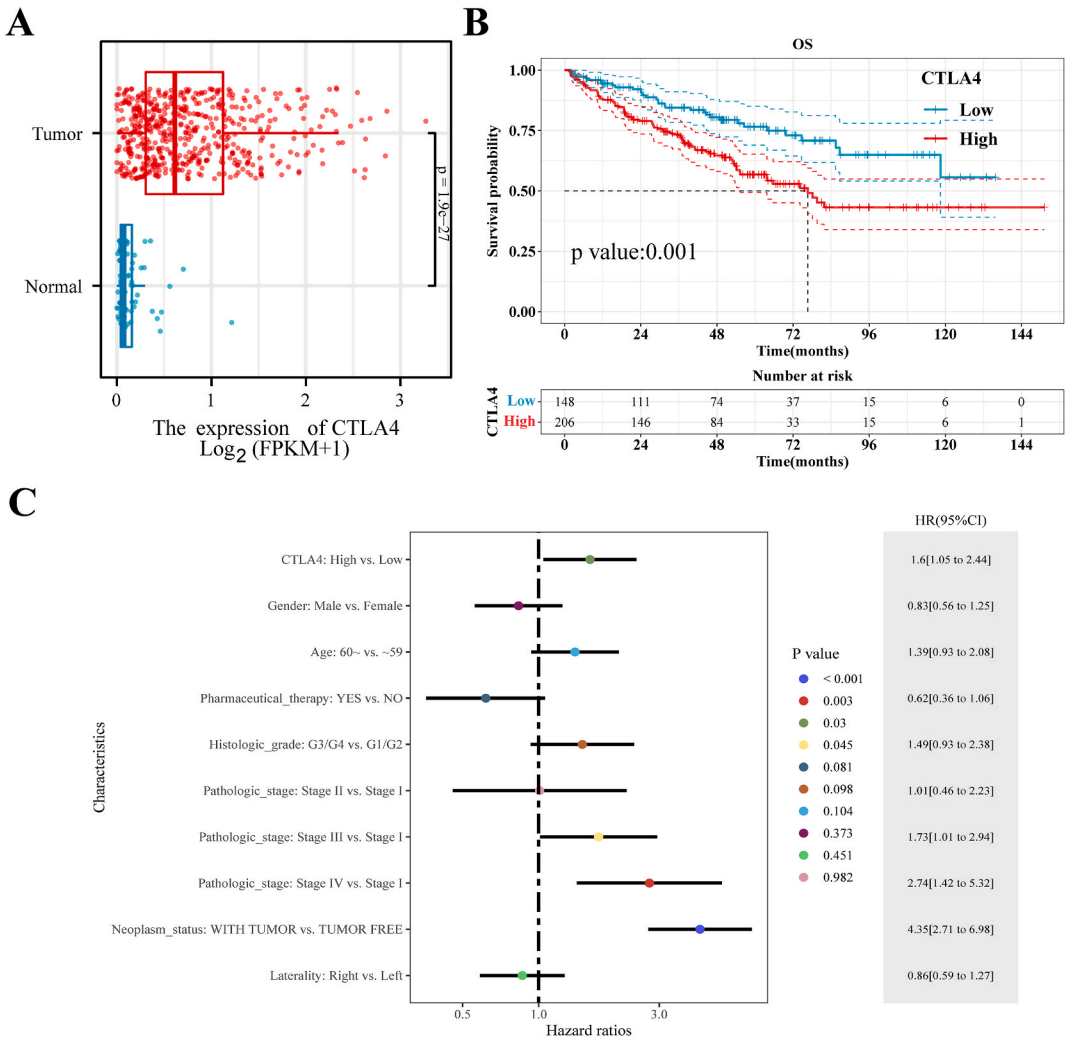

Fig. 2. CTLA4 expression was associated with poor prognosis in ccRCC. (A) CTLA4 expression in tumor and normal tissues. (B) The impact of CTLA4 expression on patient survival. (C) Univariate COX analysis of CTLA expression.

spectrophotometer (NanoDrop Technologies, Wilmington, DE, USA).

Cell migration and invasion capabilities were assessed using the Transwell assay. Caki-1 cells were seeded into the upper chambers of 24-well plates and cultured for 24 h. Subsequently, migrated cells were fixed with 4 % paraformaldehyde and stained with 0.1 % crystal violet for 30 min, followed by counting the number of migrated cells. For the invasion assay, the upper chambers were coated with Matrigel and cells were seeded into these chambers. The subsequent steps followed the aforementioned protocol, with the number of invasive cells being counted.

2.10. Quantitative reverse transcription-polymerase chain reaction (qRT-PCR)

Total RNA was extracted from cells using Trizol reagent (Invitrogen) following the manufacturer's instructions. RNA reverse transcription was performed using the SweScript RT I First Strand cDNA Synthesis Kit (Servicebio). qRT-PCR was conducted with SYBR Green qPCR Master Mix (Servicebio), and mRNA expression was normalized to GAPDH. Primer sequences are provided in Supplementary Table 1.

2.11. Western blot

Total protein lysates were extracted with RIPA buffer (Beyotime, China) and quantified using the BCA Protein Assay Kit (KeyGEN, China). Equal amounts of protein were separated by 6–12 % SDS-PAGE and transferred to PVDF membranes. After blocking, membranes were incubated with primary antibodies overnight at 4 °C, followed by incubation with secondary antibodies at room temperature for 2 h. Bands were visualized using the Bio-Rad ChemiDoc XRS system. Antibody information is listed in Supplementary Table 2.

2.12. Statistical analysis

The Wilcoxon test was employed to analyze the disparities in pathology scores between high and low CTLA4 genomes. Spearman correlation analysis was utilized to investigate the correlation between the PS and TMB. The significance test of survival rate between groups was performed using the log-rank test. All statistical analyses were conducted using R software (version 4.1.2), and a significance level of $P < 0.05$ was deemed statistically significant.

Table 1
Clinical pathological data of training set and validation set.

Variables	Total (n = 354)	Train (n = 249)	Validation (n = 105)	*P* value
CTLA4, n (%)				1
Low	148 (42)	104 (42)	44 (42)	
High	206 (58)	145 (58)	61 (58)	
Gender, n (%)				0.251
Female	111 (31)	73 (29)	38 (36)	
Male	243 (69)	176 (71)	67 (64)	
Age, n (%)				0.274
~59	176 (50)	129 (52)	47 (45)	
60~	178 (50)	120 (48)	58 (55)	
Pharmaceutical_therapy, n (%)				0.823
NO	304 (86)	215 (86)	89 (85)	
YES	50 (14)	34 (14)	16 (15)	
Histologic_grade, n (%)				0.862
G1/G2	161 (45)	112 (45)	49 (47)	
G3/G4	193 (55)	137 (55)	56 (53)	
Pathologic_stage, n (%)				0.711
Stage I	179 (51)	124 (50)	55 (52)	
Stage II	38 (11)	29 (12)	9 (9)	
Stage III	87 (25)	63 (25)	24 (23)	
Stage IV	50 (14)	33 (13)	17 (16)	
Neoplasm_status, n (%)				1
TUMOR FREE	250 (71)	176 (71)	74 (70)	
WITH TUMOR	104 (29)	73 (29)	31 (30)	
Laterality, n (%)				0.705
Left	169 (48)	121 (49)	48 (46)	
Right	185 (52)	128 (51)	57 (54)	
OS, n (%)				0.553
Alive	239 (68)	171 (69)	68 (65)	
Dead	115 (32)	78 (31)	37 (35)	
OS.time, Median (Q1,Q3)	44.1 (21.51, 63.76)	46.17 (24.23, 65.17)	36.4 (16, 62.07)	0.050

3. Results

3.1. CTLA4 is highly expressed in ccRCC and is associated with poor prognosis

In the TCGA-KIRC cohort, all samples were grouped into normal samples (n = 72) and tumor samples (n = 539). The expression of CTLA4 was significantly increased in the tumor group compared with the normal group (Fig. 2A). According to the optimal cutoff value of CTLA4, 354 samples of ccRCC patients included in the survival analysis were divided into CTLA4 high expression group (n = 206) and low expression group (n = 148). When the optimal cutoff value was 0.5046, high expression of CTLA4 led to poor outcomes in ccRCC patients (Fig. 2B), and the optimal cutoff value was obtained by using the "surfminer" package in R software. Univariate COX regression analysis of other features showed that age, pathological stage and tumor status were related to the prognosis of patients in addition to the expression level of CTLA4 (Fig. 2C).

3.2. Constructed pathomics signature

The 354 patients included in the criteria were randomly divided into a training set and a validation set. Clinical characteristics of patients with ccRCC were shown in Table 1. Our study had high efficiency in the random division, which showed no significant difference for basic clinical characteristics among training and validation sets. The training set was used to bulid the model, while the validation set was used to evaluate the model. After comparing various methods, mRMR REF was used to filter the features and 9 features were obtained (Fig. 3A). The signature result of GBM construction showed that 'log_sigma_4_0_mm_3D_glcm_InverseVariance' and 'wavelet_LL_glrlm_GrayLevelVariance' were the most important features in the model (Fig. 3B).

3.3. Verification of the pathomics signature for prediction of CTLA4 expression

Evaluating models with validation sets, ROC curve showed that this model had good sensitivity and specificity (Fig. 4A-C). In addition, the DCA curve proved that it had the potential to be used in clinical practice (Fig. 4D). The results of the training sets were shown in Supplementary Fig. 1, and the specific data of the training sets and verification sets were shown in Table 2. Subsequently, we used patient data from our clinical cohort as an external validation set, including 148 samples with CTLA4 expression data. Patients were divided into high CTLA4 expression (n = 74) and low CTLA4 expression groups (n = 74) based on the median CTLA4 expression value of 14.911. Clinical information of the patients is provided in Supplementary Table 3. For model performance evaluation, 128 samples with both pathological images and CTLA4 expression data were used. As shown by the ROC curve (Supplementary Fig. 2), the GBM model achieved an AUC value of 0.710 in the external validation set. The calibration curve indicated a good consistency between the predicted probabilities and the actual values for CTLA4 expression levels. DCA demonstrated the clinical utility of the model. All results indicated that this model had excellent predictive effects.

Pathomics score (PS) referred to the probability of predicting the level of gene expression from the output of a pathological model. All patients were divided into high PS group and low PS group according to the optimal cut-off value of PS. The best cutoff value for PS was 0.582, which was obtained from the "surviminer" package in R software. In the KM plot, the median survival time of the high PS group was 79.53 months, while the low PS group did not reach the median survival time due to the low number of deaths. The Survival curve of high and low PS displayed that high PS was significantly correlated with the deterioration of overall survival (OS) ($P < 0.001$) (Fig. 4 E).

In the validation sets, the PS score of the CTLA4 high expression group was significantly increased compared with the CTLA4 low expression group (Fig. 4F). Consistent results were observed in both the training set and the external validation set (Supplementary Figs. 1 and 2). Univariate COX analysis showed a high value of PS was a statistically significant risk factor for OS (HR = 2.08, 95 % CI 1.39–3.11, $P < 0.001$) (Fig. 4G).

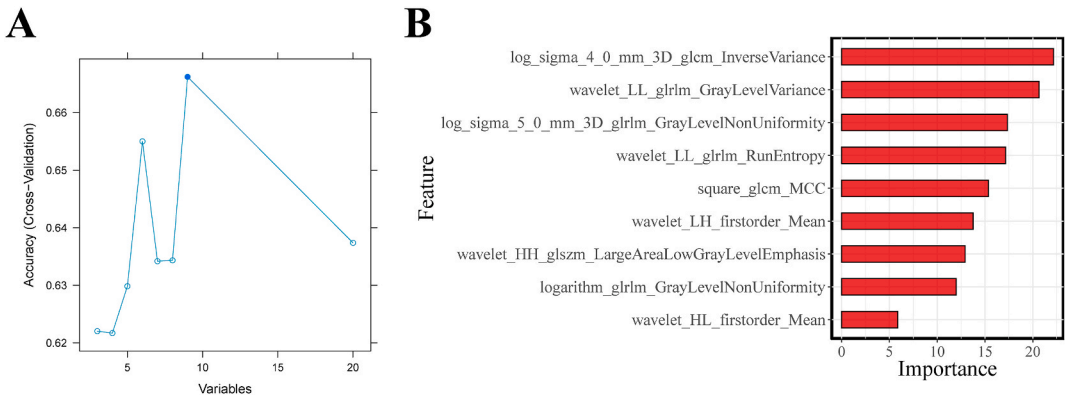

Fig. 3. Construction of the pathomics signature. (A) Feature selection in machine learning. (B) The importance of features in GBM algorithms.

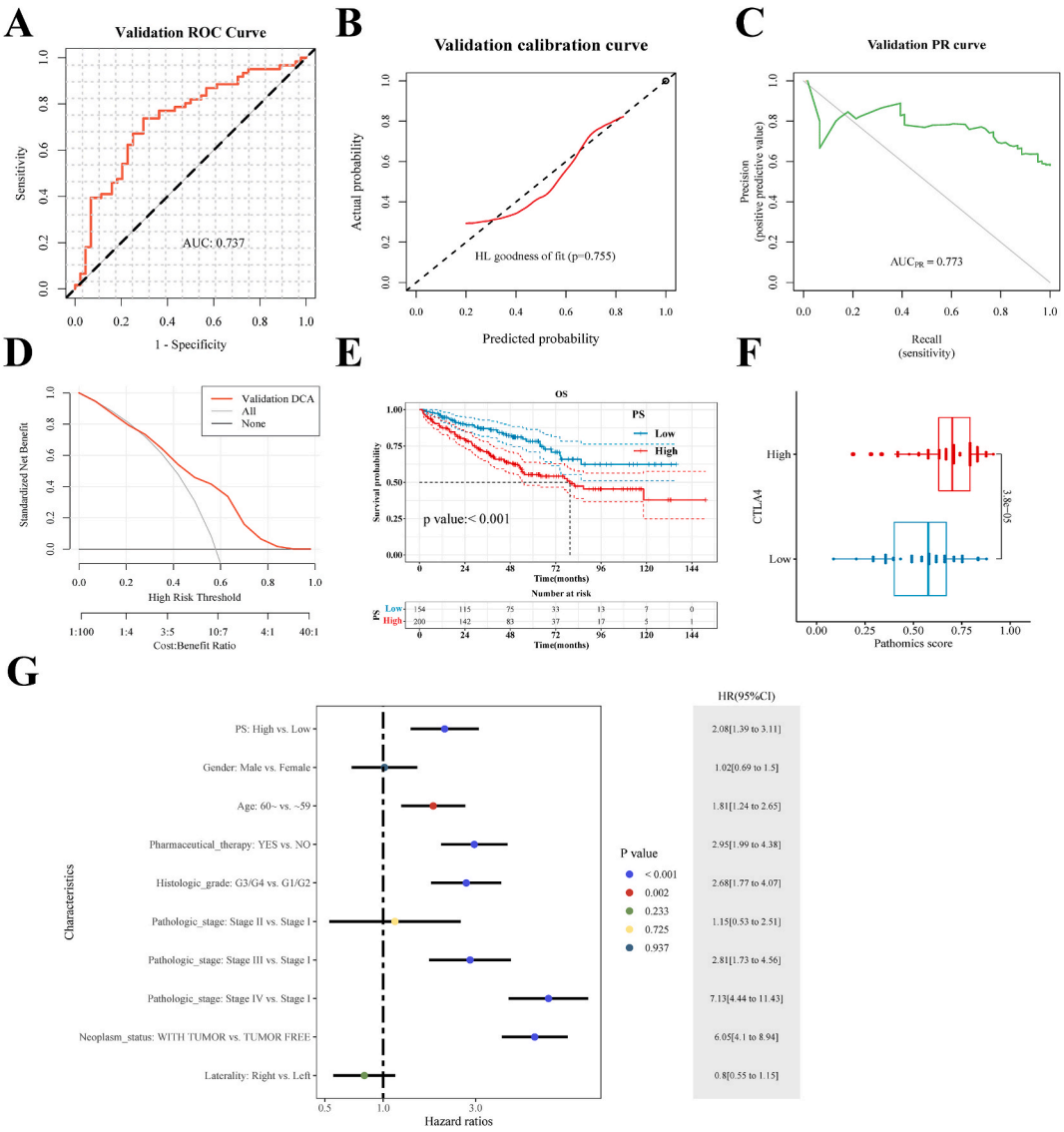

Fig. 4. Comprehensive evaluation of the pathomics signature in the validation set and its predictive ability for CTLA4 expression. (A) ROC curve. (B) Calibration curve. (C) PR curve. (D) DCA curve. (E) Survival curve of high and low PS. (F) PS in high and low CTLA4 expression groups. (G) Univariate COX analysis of PS.

Table 2
Evaluation parameters of pathomics signatures.

	Accuracy	Sensitivity	Specificity	PPV	NPV
Training Set	0.775	0.821	0.712	0.799	0.74
Validation Set	0.724	0.738	0.705	0.776	0.66

NPV: Negative predictive value; PPV: Positive predictive value.

3.4. Mechanism analysis of pathomics signature

The differentially expressed genes (DEG) found in high and low PS groups were analyzed by Gene Set Enrichment Analysis (GSEA) in KEGG database (Fig. 5A) and HALLMARK database (Fig. 5B). In the KEGG database, DEGs in the PS high expression group were significantly enriched in the TGF-β (TGF_BETA_SIGNALING_PATHWAY) signalling pathway, and in the HALLMARK database, DEG in the PS high expression group was also significantly enriched in the TGF-β (TGF_BETA_SIGNALING_PATHWAY) signalling pathway. This result suggested that PS expression levels may be related to the TGF-β signalling pathway. The spearman correlation analysis

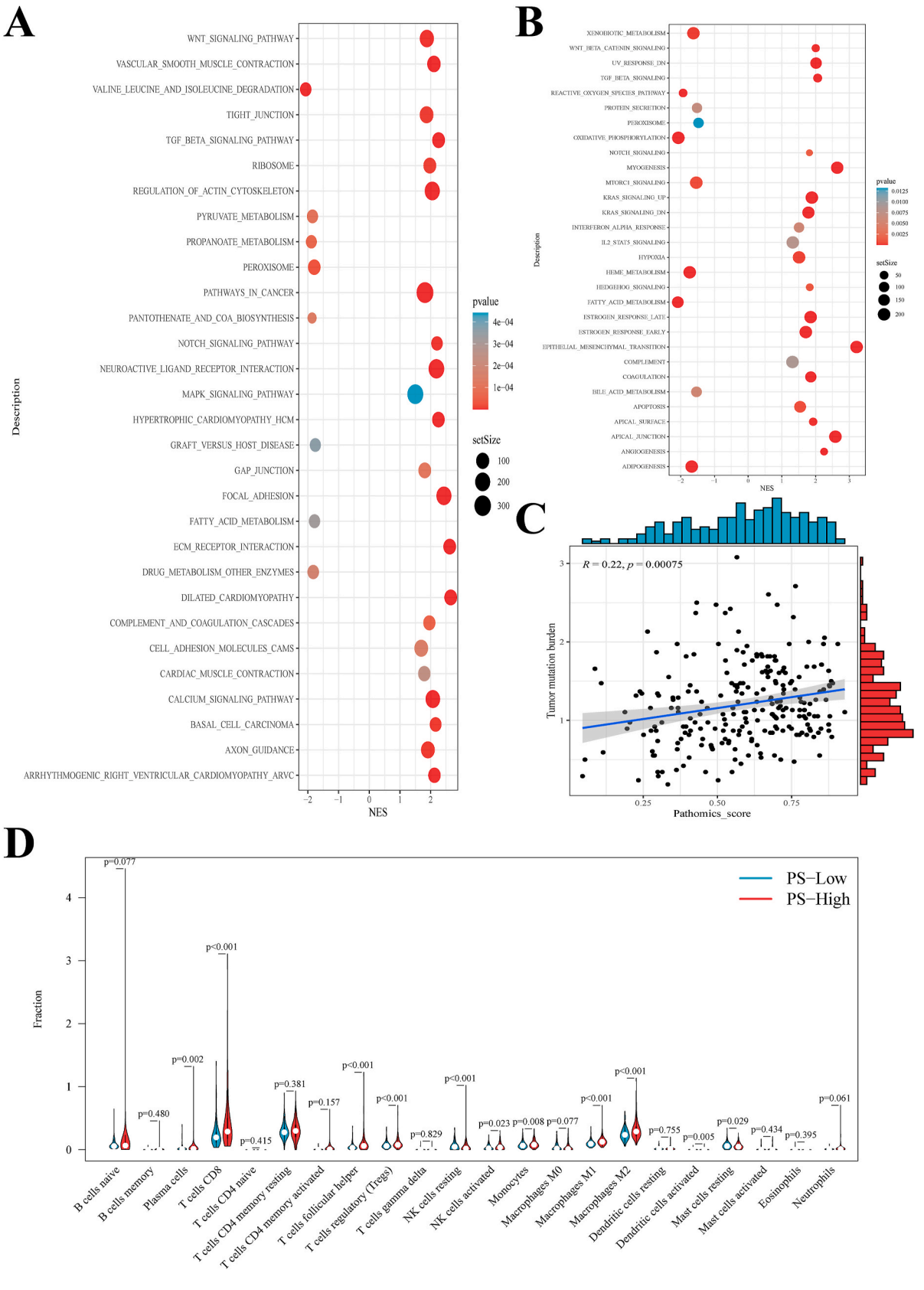

(caption on next page)

Fig. 5. The molecular mechanisms underlying the pathomics signature. (A) GSEA in KEGG database. (B) GSEA in HALLMARK database. (C) Correlation between pathomics score and TMB. (D) Pathomics score and immune infiltration analysis in CIBERSORT database.

displayed that PS was significantly positively correlated with TMB ($P < 0.001$) (Fig. 5C). The infiltration analysis of immune cells in ccRCC showed that the infiltration of T cell regulatory (Tregs), Macrophage M1 and macrophage M2 were higher in the high PS group ($P < 0.001$) (Fig. 5D). In recent years, the combined inhibition of PD-L1 and CTLA4 has garnered widespread attention. Therefore, we further investigated the correlation between CTLA4 and PD-1 (encoded by PDCD1) and PD-L1 (encoded by CD274) in patients with clear cell renal cell carcinoma. Our findings revealed a pronounced positive correlation between CTLA4 and both PD-1 and PD-L1 (Supplementary Fig. 3, $p < 0.001$).

3.5. *Impact and mechanistic verification of CTLA4 on the proliferation, migration, and invasion of ccRCC cells in vitro*

In order to further elucidate the role of CTLA4 in ccRCC, we assessed whether alterations in CTLA4 expression would influence the proliferation of ccRCC cells. Transfection of siCTLA4 was performed, and subsequent qRT-PCR and Western blot (WB) analyses confirmed CTLA4 knockdown (Fig. 6A and B). The CCK-8 assay results demonstrated that downregulation of CTLA4 expression inhibited cell proliferation (Fig. 6C). The role of CTLA4 in cell invasion and migration was examined using Transwell assays, and the results showed that CTLA4 knockdown suppressed the migration and invasion of Caki-1 cells (Fig. 6D). To further validate the relationship between CTLA4 and the TGF-β signaling pathway, as well as macrophage polarization, qRT-PCR and WB analyses were employed to assess the impact of CTLA4 knockdown on the expression of TGF-β, iNOS, and CD206. The results revealed a significant suppression of TGF-β expression by siCTLA4. Moreover, compared to the negative control (NC) group, macrophages co-cultured with siCTLA4 ccRCC cells exhibited elevated levels of M1-like marker iNOS and reduced levels of M2-like marker CD206 (Fig. 6E–G). These findings suggest that CTLA4 knockdown inhibits cell proliferation, downregulates TGF-β expression, and impedes the M2-type

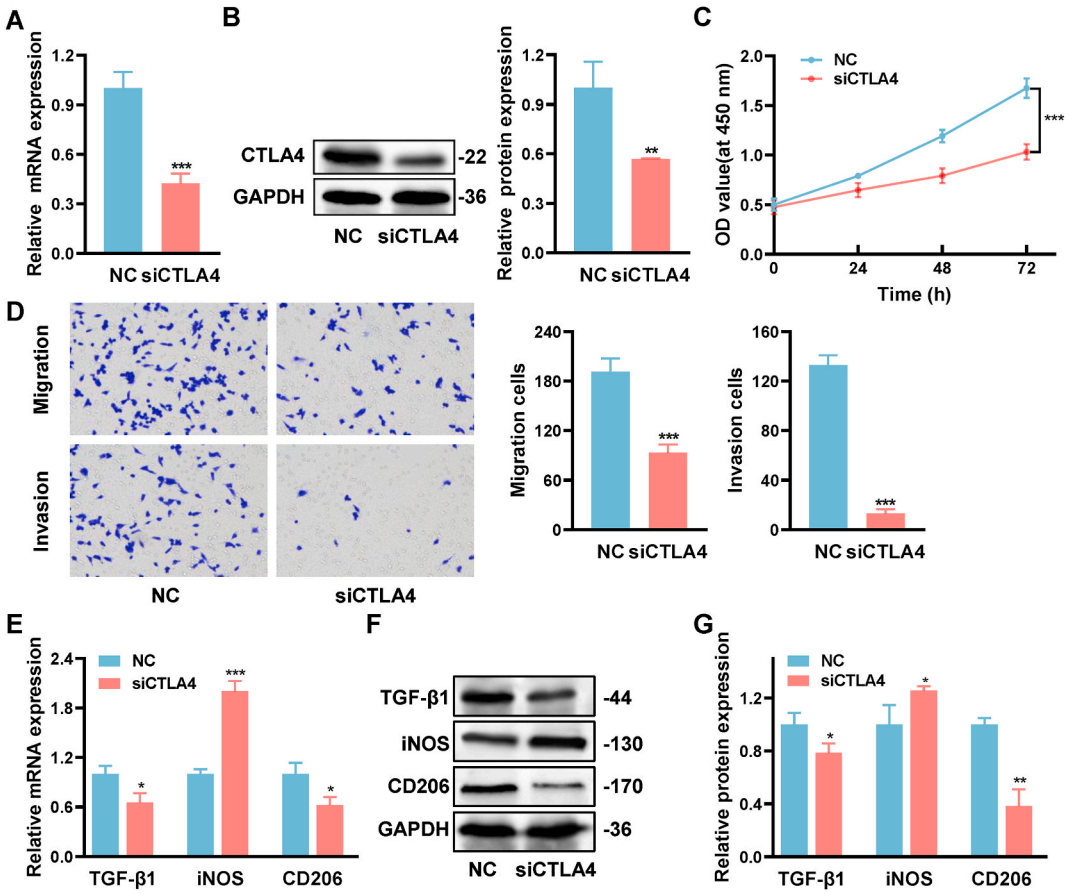

Fig. 6. Impact and mechanistic verification of CTLA4 on ccRCC Cell proliferation, migration, and invasion *in vitro*. (A–B) qRT-PCR and Western blot analyses were performed to assess the expression levels of CTLA4 in Caki1 cells transfected with small interfering RNA (siRNA) targeting CTLA4 and control siRNA. (C) Cell proliferation was evaluated using the Cell Counting Kit-8 (CCK-8) assay. (D) Transwell assay showing cell migration and invasion. (E–G) Following co-cultivation of transfected cells, qRT-PCR and Western blot analyses were conducted to measure the expression levels of iNOS and CD206 in macrophages. The unedited images are referenced in Supplementary Fig. 4. *P < 0.05, **P < 0.01, ***P < 0.001 *vs* NC group.

polarization of macrophages.

4. Discussion

ccRCC patients have a poor postoperative prognosis [2], and biomarkers play a significant role in assessing treatment efficacy and prognosis of tumors. Currently, the field of oncology emphasizes the effectiveness of cancer immunotherapy in cancer treatment [24]. It is noteworthy that immune checkpoint molecules such as PD-L1 and CTLA4 are considered critical regulatory factors in immune response, holding promise as potential stratified prognostic biomarkers in certain cancer types, including ccRCC [11,12,25]. Targeting immune checkpoint inhibitors against PD-1, PD-L1, and CTLA4 has garnered the highest attention and widespread research in the realm of immunotherapy for ccRCC patients [26]. The role of anti-CTLA4 agents in the immunotherapeutic landscape of ccRCC patients is of paramount significance, and our previous endeavors have encompassed a series of investigations into the molecular aspects of CTLA4 [12]. As a further exploration of the preliminary research, a pathomics-based PS signature was developed to predict the expression level of CTLA4 and its overall survival in ccRCC patients. Further enrichment analysis and immune infiltration analysis showed that DEGs in the PS high expression group were significantly enriched in the TGF-β signaling pathway and significantly correlated with TMB and immune infiltration.

CTLA4 is a crucial transmembrane receptor on T cells that competes with CD28 for the B7 molecular ligand. Its binding to the ligand transmits inhibitory signals to T cells, promoting tumor cell growth [27]. Previous evidence suggests that the expression level of CTLA4 is crucial for the survival and prognosis of cancer patients. According to recent literature, CTLA4 is overexpressed in various hematological malignancies, which is associated with poor survival rates [28]. Targeted drugs that block CTLA4, such as Ipilimumab, have been demonstrated to improve OS in patients with renal cell carcinoma [29,30], and advanced non-small cell lung cancer [31]. A pan-cancer analysis revealed that CTLA4, as a biomarker, exhibits high expression in certain cancer types, including ccRCC, and correlates positively with clinical staging and microenvironment scoring, indicating a high prognostic value [10]. Consistent with our preliminary work [12], our research findings also indicate high expression of CTLA4 in ccRCC tissue, potentially leading to unfavorable prognosis. This observation has been validated *in vitro* using ccRCC cells, where downregulation of CTLA4 expression was found to suppress the proliferation of ccRCC cells.

The expression level of CTLA4 can be assessed using various methods. Firstly, peripheral blood detection methods such as ELISA [15] can be employed, but they have limitations, including real-time detection constraints, high cost, and an inability to reflect tumor parenchyma. Secondly, fresh tissue specimens can be used for detection, involving qRT-PCR at the RNA level, Western blot, or flow cytometry at the protein level. However, specimen collection can be challenging, and detection can be influenced by operators and antibodies. Thirdly, paraffin tissue samples can be utilized for detection using techniques such as immunohistochemistry, immunofluorescence, and high-throughput sequencing [32]. However, these methods also have their own drawbacks, including reliance on operators, variability in antibodies, and high costs. Notably, clinical diagnosis requires H&E staining sections, which represent the most accessible image data. The field of pathology has experienced significant changes with the introduction of artificial intelligence, which is gradually being applied to aid pathologists. In this study, we aimed to address these limitations and fill the existing gap. Initially, we collected histopathological images from a large cohort of ccRCC patients and extracted features using the TCGA database. Subsequently, machine learning techniques such as mRMR, REF, and GBM were employed to construct a pathomics signature. The resulting model was extensively validated. Our findings demonstrate that this model not only accurately predicts patient prognosis but also reflects CTLA4 expression levels, potentially reducing the need for additional costly examinations in clinical practice.

Additionally, CTLA4 inhibitors have been shown to increase T cell growth by depleting Tregs. In our preliminary research, it has also been demonstrated that CTLA4 promotes tumor growth by facilitating immune evasion [12]. In this study, we further validate that the level of PS can impact the expression of Tregs, which can induce immune suppression through contact-dependent mechanisms or contact-independent mechanisms, including the generation of soluble immunosuppressive molecules such as TGF-β [33]. Furthermore, the high expression of CTLA4 in cancers such as ccRCC is strongly associated with immune subtypes C2 (IFN-γ dominant) and C6 (TGF-β dominant) [10]. Our data indicate a significant correlation between high PS expression and the TGF-β pathway. The validation of our findings was further substantiated through *in vitro* experiments involving ccRCC cells. Consistently, the downregulation of CTLA4 was concomitant with a notable reduction in the expression of TGF-β. The observed correlation not only reinforces the pivotal role of CTLA4 in immune modulation but also unveils a potential mechanistic link to TGF-β-mediated signaling pathways in the context of ccRCC. On the other hand, the expression of CTLA4 in immune infiltration of ccRCC tumors has been found to be correlated with patient prognosis, with higher CTLA4 expression indicating worse outcomes [34,35]. The CTLA4 and PD-L1 pathways represent pivotal targets in immunotherapy, and our data elucidate a conspicuous positive correlation between CTLA4 and both PD-1 and PD-L1. This observation aligns seamlessly with previous investigations in the realm of cancer research. Jiang et al. demonstrated a positive correlation between PD-L1 and CTLA4 expression in breast cancer, underscoring the consistency of our findings [36]. Similarly, Liu et al. identified a positive correlation between PD1 and CTLA4 expression in glioma patients across diverse populations [37]. The contemporary landscape of cancer therapy has witnessed a paradigm shift, notably with the combined application of CTLA4 and PD-1 inhibitors, demonstrating an augmentation in the rate of remission among cancer patients [38]. This compelling evidence further underscores the synergistic role of CTLA4 in conjunction with PD-1/PD-L1 in shaping the prognosis of tumors. Collectively, these findings strongly suggest that CTLA4 may play a pivotal role in the occurrence of clear cell renal carcinoma and the orchestration of immune regulatory processes. Furthermore, it is plausible that CTLA4 could exert influence on immune cell infiltration dynamics and consequently impact the outcomes of immune-based therapeutic interventions.

In addition, our study revealed that the high PS group with adverse prognoses exhibited elevated expression levels of both macrophage M1 and M2 subtypes. Consistent with our findings, previous research has indicated that macrophage M2 subtype can

suppress inflammatory responses, induce angiogenesis, and participate in tumor initiation and progression, posing a risk factor for unfavorable outcomes in ccRCC patients [39]. Macrophage M1, on the other hand, demonstrates anti-tumor characteristics due to its intrinsic phagocytic activity and enhanced anti-tumor inflammatory response [40]. The interconversion of M1 and M2 macrophages under specific signals has been reported [39], possibly accounting for the simultaneous elevation of both subtypes observed in our study. Similarly, in a prognostic model for glioma patients developed by Jiang et al. [41], both macrophage M1 and M2 showed an increasing trend, highly correlated with CTLA4, and the expression levels were significantly elevated in the high-risk group. Furthermore, recent studies have suggested that the M1/M2 ratio may serve as a more robust biomarker for survival outcomes [42]. In line with this, downregulating CTLA4 was demonstrated to prevent macrophage polarization towards the M2 subtype. Collectively, these findings underscore the critical role of CTLA4 in promoting M2 activation and immune suppression, suggesting that targeted inhibition of CTLA4 holds promise for enhancing the efficacy of immunotherapy in treating tumors. Over the years, research on the prognosis prediction of tumor patients has evolved from single-gene analyses to encompass multiple omics signatures. ccRCC is a prominent area of study, and our research group previously developed a radiomics signature for ccRCC patients [12]. The results demonstrated that the radiomics signature effectively predicts CTLA4 expression and patient prognosis in ccRCC cases, consistent with the findings of this study's pathomics signature. However, it is important to note that these models are based on limited sample sizes, relying on predictions from public databases. Future studies should aim to include a larger number of patient samples to continuously refine and improve the model.

5. Conclusion

In conclusion, our study provides valuable insights into the significance of CTLA4 in the prognosis of ccRCC and highlights the potential of employing pathomics signatures in clinical practice. We established a pathomics signature using machine learning to predict patient prognosis and demonstrate its correlation with CTLA4 expression levels, indicating its potential as a cost-effective instrument in clinical practice. Nonetheless, further studies involving larger patient cohorts are necessary to enhance the reliability and applicability of the model.

Data availability statement

The datasets used and/or analyzed during the current study available from the corresponding author on reasonable request.

Ethics statement

This research was conducted in compliance with the principles outlined in the Declaration of Helsinki and received ethical approval from the Institutional Review Board of Shanghai Ruijin Hospital, Shanghai Jiaotong University School of Medicine (KY2020-322). Due to the anonymity of patient data, the need for informed consent was waived.

Funding

This work was supported by grants from the National Natural Science Foundation of China (No. 82372724).

CRediT authorship contribution statement

Xiaoqun Yang: Writing – original draft, Validation, Project administration, Methodology, Conceptualization. **Xiangyun Li:** Writing – original draft, Validation, Project administration, Methodology, Conceptualization. **Haimin Xu:** Writing – original draft, Validation, Project administration, Methodology, Conceptualization. **Silin Du:** Validation, Software, Formal analysis, Data curation. **Chaofu Wang:** Writing – review & editing, Supervision. **Hongchao He:** Writing – review & editing, Supervision.

Declaration of competing interest

The authors declare that they have no known competing financial interests or personal relationships that could have appeared to influence the work reported in this paper.

Acknowledgement

We thank Ms. Ivy from Shanghai Hover International Education for her assistance with language editing.

Appendix A. Supplementary data

Supplementary data to this article can be found online at https://doi.org/10.1016/j.heliyon.2024.e34877.

References

[1] L. Bukavina, K. Bensalah, F. Bray, M. Carlo, B. Challacombe, J.A. Karam, W. Kassouf, T. Mitchell, R. Montironi, T. O'Brien, V. Panebianco, G. Scelo, B. Shuch, H. van Poppel, C.D. Blosser, S.P. Psutka, Epidemiology of renal cell carcinoma: 2022 update, Eur. Urol. 82 (2022) 529–542, https://doi.org/10.1016/j.eururo.2022.08.019.

[2] Q. Deng, Y. Du, Z. Wang, Y. Chen, J. Wang, H. Liang, D. Zhang, Identification and validation of a DNA methylation-driven gene-based prognostic model for clear cell renal cell carcinoma, BMC Genom. 24 (2023) 307, https://doi.org/10.1186/s12864-023-09416-z.

[3] S. Mazumder, P.J. Higgins, R. Samarakoon, Downstream targets of VHL/HIF-alpha signaling in renal clear cell carcinoma progression: mechanisms and therapeutic relevance, Cancers 15 (2023) 1316, https://doi.org/10.3390/cancers15041316.

[4] W.G. Kaelin Jr., Von Hippel-Lindau disease: insights into oxygen sensing, protein degradation, and cancer, J. Clin. Invest. 132 (2022) e162480, https://doi.org/10.1172/JCI162480.

[5] L. Carril-Ajuria, M. Santos, J.M. Roldan-Romero, C. Rodriguez-Antona, G. de Velasco, Prognostic and predictive value of PBRM1 in clear cell renal cell carcinoma, Cancers 12 (2019) 16, https://doi.org/10.3390/cancers12010016.

[6] A.M. Alchahin, S. Mei, I. Tsea, T. Hirz, Y. Kfoury, D. Dahl, C.L. Wu, A.O. Subtelny, S. Wu, D.T. Scadden, J.H. Shin, P.J. Saylor, D.B. Sykes, P.V. Kharchenko, N. Baryawno, A transcriptional metastatic signature predicts survival in clear cell renal cell carcinoma, Nat. Commun. 13 (2022) 5747, https://doi.org/10.1038/s41467-022-33375-w.

[7] X. Yin, Z. Wang, J. Wang, Y. Xu, W. Kong, J. Zhang, Development of a novel gene signature to predict prognosis and response to PD-1 blockade in clear cell renal cell carcinoma, OncoImmunology 10 (2021) 1933332, https://doi.org/10.1080/2162402X.2021.1933332.

[8] B.H. Cotta, T.K. Choueiri, M. Cieslik, P. Ghatalia, R. Mehra, T.M. Morgan, G.S. Palapattu, B. Shuch, U. Vaishampayan, E. Van Allen, A. Ari Hakimi, S.S. Salami, Current landscape of genomic biomarkers in clear cell renal cell carcinoma, Eur. Urol. 84 (2023) 166–175, https://doi.org/10.1016/j.eururo.2023.04.003.

[9] D. Miao, C.A. Margolis, W. Gao, M.H. Voss, W. Li, D.J. Martini, C. Norton, D. Bosse, S.M. Wankowicz, D. Cullen, C. Horak, M. Wind-Rotolo, A. Tracy, M. Giannakis, F.S. Hodi, C.G. Drake, M.W. Ball, M.E. Allaf, A. Snyder, M.D. Hellmann, T. Ho, R.J. Motzer, S. Signoretti, W.G. Kaelin Jr., T.K. Choueiri, E.M. Van Allen, Genomic correlates of response to immune checkpoint therapies in clear cell renal cell carcinoma, Science 359 (2018) 801–806, https://doi.org/10.1126/science.aan5951.

[10] Z. Cai, X. Ang, Z. Xu, S. Li, J. Zhang, C. Pei, F. Zhou, A pan-cancer study of PD-1 and CTLA-4 as therapeutic targets, Transl. Cancer Res. 10 (2021) 3993–4001, https://doi.org/10.21037/tcr-21-561.

[11] B. Rowshanravan, N. Halliday, D.M. Sansom, CTLA-4: a moving target in immunotherapy, Blood 131 (2018) 58–67, https://doi.org/10.1182/blood-2017-06-741033.

[12] H. He, Z. Jin, J. Dai, H. Wang, J. Sun, D. Xu, Computed tomography-based radiomics prediction of CTLA4 expression and prognosis in clear cell renal cell carcinoma, Cancer Med. 12 (2023) 7627–7638, https://doi.org/10.1002/cam4.5449.

[13] K. Shitara, J.A. Ajani, M. Moehler, M. Garrido, C. Gallardo, L. Shen, K. Yamaguchi, L. Wyrwicz, T. Skoczylas, A.C. Bragagnoli, T. Liu, M. Tehfe, E. Elimova, R. Bruges, T. Zander, S. de Azevedo, R. Kowalyszyn, R. Pazo-Cid, M. Schenker, J.M. Cleary, P. Yanez, K. Feeney, M.V. Karamouzis, V. Poulart, M. Lei, H. Xiao, K. Kondo, M. Li, Y.Y. Janjigian, Nivolumab plus chemotherapy or ipilimumab in gastro-oesophageal cancer, Nature 603 (2022) 942–948, https://doi.org/10.1038/s41586-022-04508-4.

[14] A. Zhang, Z. Ren, K.F. Tseng, X. Liu, H. Li, C. Lu, Y. Cai, J.D. Minna, Y.X. Fu, Dual targeting of CTLA-4 and CD47 on T(reg) cells promotes immunity against solid tumors, Sci. Transl. Med. 13 (2021) eabg8693, https://doi.org/10.1126/scitranslmed.abg8693.

[15] M.K. Misra, A. Mishra, S.R. Phadke, S. Agrawal, Association of functional genetic variants of CTLA4 with reduced serum CTLA4 protein levels and increased risk of idiopathic recurrent miscarriages, Fertil. Steril. 106 (2016) 1115–1123 e1116, https://doi.org/10.1016/j.fertnstert.2016.06.011.

[16] K. Liu, J. Hu, Classification of acute myeloid leukemia M1 and M2 subtypes using machine learning, Comput. Biol. Med. 147 (2022) 105741, https://doi.org/10.1016/j.compbiomed.2022.105741.

[17] M. Nishio, M. Nishio, N. Jimbo, K. Nakane, Homology-based image processing for automatic classification of histopathological images of lung tissue, Cancers 13 (2021) 1192, https://doi.org/10.3390/cancers13061192.

[18] G.L. Banna, T. Olivier, F. Rundo, U. Malapelle, F. Fraggetta, M. Libra, A. Addeo, The promise of digital biopsy for the prediction of tumor molecular features and clinical outcomes associated with immunotherapy, Front. Med. 6 (2019) 172, https://doi.org/10.3389/fmed.2019.00172.

[19] L. Chen, H. Zeng, M. Zhang, Y. Luo, X. Ma, Histopathological image and gene expression pattern analysis for predicting molecular features and prognosis of head and neck squamous cell carcinoma, Cancer Med. 10 (2021) 4615–4628, https://doi.org/10.1002/cam4.3965.

[20] H. Zeng, L. Chen, M. Zhang, Y. Luo, X. Ma, Integration of histopathological images and multi-dimensional omics analyses predicts molecular features and prognosis in high-grade serous ovarian cancer, Gynecol. Oncol. 163 (2021) 171–180, https://doi.org/10.1016/j.ygyno.2021.07.015.

[21] X. Wang, H. Chen, C. Gan, H. Lin, Q. Dou, E. Tsougenis, Q. Huang, M. Cai, P.A. Heng, Weakly supervised deep learning for whole slide lung cancer image analysis, IEEE Trans. Cybern. 50 (2020) 3950–3962, https://doi.org/10.1109/TCYB.2019.2935141.

[22] K. Saednia, A. Lagree, M.A. Alera, L. Fleshner, A. Shiner, E. Law, B. Law, D.W. Dodington, F.I. Lu, W.T. Tran, A. Sadeghi-Naini, Quantitative digital histopathology and machine learning to predict pathological complete response to chemotherapy in breast cancer patients using pre-treatment tumor biopsies, Sci. Rep. 12 (2022) 9690, https://doi.org/10.1038/s41598-022-13917-4.

[23] H. Li, L. Chen, H. Zeng, Q. Liao, J. Ji, X. Ma, Integrative analysis of histopathological images and genomic data in colon adenocarcinoma, Front. Oncol. 11 (2021) 636451, https://doi.org/10.3389/fonc.2021.636451.

[24] Q. Wang, H. Tang, X. Luo, J. Chen, X. Zhang, X. Li, Y. Li, Y. Chen, Y. Xu, S. Han, Immune-associated gene signatures serve as a promising biomarker of immunotherapeutic prognosis for renal clear cell carcinoma, Front. Immunol. 13 (2022) 890150, https://doi.org/10.3389/fimmu.2022.890150.

[25] H. Zhang, Z. Dai, W. Wu, Z. Wang, N. Zhang, L. Zhang, W.J. Zeng, Z. Liu, Q. Cheng, Regulatory mechanisms of immune checkpoints PD-L1 and CTLA-4 in cancer, J. Exp. Clin. Cancer Res. 40 (2021) 184, https://doi.org/10.1186/s13046-021-01987-7.

[26] Y.F. Liu, Z.C. Zhang, S.Y. Wang, S.Q. Fu, X.F. Cheng, R. Chen, T. Sun, Immune checkpoint inhibitor-based therapy for advanced clear cell renal cell carcinoma: a narrative review, Int. Immunopharm. 110 (2022) 108900, https://doi.org/10.1016/j.intimp.2022.108900.

[27] C. Rudd, The reverse stop-signal model for CTLA4 function, Nat. Rev. Immunol. 8 (2008) 153–160.

[28] M. Sadeghi, A. Khodakarami, A. Ahmadi, M. Fathi, J. Gholizadeh Navashenaq, H. Mohammadi, M. Yousefi, M. Hojjat-Farsangi, A.A. Movasaghpour Akbari, F. Jadidi-Niaragh, The prognostic and therapeutic potentials of CTLA-4 in hematological malignancies, Expert Opin. Ther. Targets 26 (2022) 1057–1071, https://doi.org/10.1080/14728222.2022.2170781.

[29] D. Cella, V. Grunwald, B. Escudier, H.J. Hammers, S. George, P. Nathan, M.O. Grimm, B.I. Rini, J. Doan, C. Ivanescu, J. Paty, S. Mekan, R.J. Motzer, Patient-reported outcomes of patients with advanced renal cell carcinoma treated with nivolumab plus ipilimumab versus sunitinib (CheckMate 214): a randomised, phase 3 trial, Lancet Oncol. 20 (2019) 297–310, https://doi.org/10.1016/S1470-2045(18)30778-2.

[30] R.J. Motzer, N.M. Tannir, D.F. McDermott, O. Aren Frontera, B. Melichar, T.K. Choueiri, E.R. Plimack, P. Barthelemy, C. Porta, S. George, T. Powles, F. Donskov, V. Neiman, C.K. Kollmannsberger, P. Salman, H. Gurney, R. Hawkins, A. Ravaud, M.O. Grimm, S. Bracarda, C.H. Barrios, Y. Tomita, D. Castellano, B.I. Rini, A. C. Chen, S. Mekan, M.B. McHenry, M. Wind-Rotolo, J. Doan, P. Sharma, H.J. Hammers, B. Escudier, I. CheckMate, Nivolumab plus ipilimumab versus sunitinib in advanced renal-cell carcinoma, N. Engl. J. Med. 378 (2018) 1277–1290, https://doi.org/10.1056/NEJMoa1712126.

[31] M.D. Hellmann, L. Paz-Ares, B. Bernabe Caro, B. Zurawski, S.W. Kim, E. Carcereny Costa, K. Park, A. Alexandru, L. Lupinacci, E. de la Mora Jimenez, H. Sakai, I. Albert, A. Vergnenegre, S. Peters, K. Syrigos, F. Barlesi, M. Reck, H. Borghaei, J.R. Brahmer, K.J. O'Byrne, W.J. Geese, P. Bhagavatheeswaran, S.K. Rabindran, R.S. Kasinathan, F.E. Nathan, S.S. Ramalingam, Nivolumab plus ipilimumab in advanced non-small-cell lung cancer, N. Engl. J. Med. 381 (2019) 2020–2031, https://doi.org/10.1056/NEJMoa1910231.

[32] X.J. Guo, J.C. Lu, H.Y. Zeng, R. Zhou, Q.M. Sun, G.H. Yang, Y.Z. Pei, X.L. Meng, Y.H. Shen, P.F. Zhang, J.B. Cai, P.X. Huang, A.W. Ke, Y.H. Shi, J. Zhou, J. Fan, Y. Chen, L.X. Yang, G.M. Shi, X.Y. Huang, CTLA-4 synergizes with PD1/PD-L1 in the inhibitory tumor microenvironment of intrahepatic cholangiocarcinoma, Front. Immunol. 12 (2021) 705378, https://doi.org/10.3389/fimmu.2021.705378.

[33] A.J. Oweida, L. Darragh, A. Phan, D. Binder, S. Bhatia, A. Mueller, B.V. Court, D. Milner, D. Raben, R. Woessner, L. Heasley, R. Nemenoff, E. Clambey, S. D. Karam, STAT3 modulation of regulatory T cells in response to radiation therapy in head and neck cancer, J. Natl. Cancer Inst. 111 (2019) 1339–1349, https://doi.org/10.1093/jnci/djz036.
[34] S. Zhang, E. Zhang, J. Long, Z. Hu, J. Peng, L. Liu, F. Tang, L. Li, Y. Ouyang, Z. Zeng, Immune infiltration in renal cell carcinoma, Cancer Sci. 110 (2019) 1564–1572, https://doi.org/10.1111/cas.13996.
[35] J.N. Liu, X.S. Kong, T. Huang, R. Wang, W. Li, Q.F. Chen, Clinical implications of aberrant PD-1 and CTLA4 expression for cancer immunity and prognosis: a pan-cancer study, Front. Immunol. 11 (2020) 2048, https://doi.org/10.3389/fimmu.2020.02048.
[36] C. Jiang, S. Cao, N. Li, L. Jiang, T. Sun, PD-1 and PD-L1 correlated gene expression profiles and their association with clinical outcomes of breast cancer, Cancer Cell Int. 19 (2019) 233, https://doi.org/10.1186/s12935-019-0955-2.
[37] F. Liu, J. Huang, X. Liu, Q. Cheng, C. Luo, Z. Liu, CTLA-4 correlates with immune and clinical characteristics of glioma, Cancer Cell Int. 20 (2020) 7, https://doi.org/10.1186/s12935-019-1085-6.
[38] A. Rotte, Combination of CTLA-4 and PD-1 blockers for treatment of cancer, J. Exp. Clin. Cancer Res. 38 (2019) 255, https://doi.org/10.1186/s13046-019-1259-z.
[39] H. Shen, J. Liu, S. Chen, X. Ma, Y. Ying, J. Li, W. Wang, X. Wang, L. Xie, Prognostic value of tumor-associated macrophages in clear cell renal cell carcinoma: a systematic review and meta-analysis, Front. Oncol. 11 (2021) 657318, https://doi.org/10.3389/fonc.2021.657318.
[40] J. Liu, X. Geng, J. Hou, G. Wu, New insights into M1/M2 macrophages: key modulators in cancer progression, Cancer Cell Int. 21 (2021) 389, https://doi.org/10.1186/s12935-021-02089-2.
[41] F. Jiang, F. Luo, N. Zeng, Y. Mao, X. Tang, J. Wang, Y. Hu, C. Wu, Characterization of fatty acid metabolism-related genes landscape for predicting prognosis and aiding immunotherapy in glioma patients, Front. Immunol. 13 (2022) 902143, https://doi.org/10.3389/fimmu.2022.902143.
[42] X. Yuan, J. Zhang, D. Li, Y. Mao, F. Mo, W. Du, X. Ma, Prognostic significance of tumor-associated macrophages in ovarian cancer: a meta-analysis, Gynecol. Oncol. 147 (2017) 181–187, https://doi.org/10.1016/j.ygyno.2017.07.007.